

## Mechanism to Generate a Two-Dimensional Electron Gas at the Surface of the Charge-Ordered Semiconductor BaBiO<sub>3</sub>

Verónica Vildosola,<sup>1</sup> Francisco Güller,<sup>1,2</sup> and Ana María Llois<sup>1,2</sup>

<sup>1</sup>*Departamento de Materia Condensada, Gerencia de Investigación y Aplicaciones, Comisión Nacional de Energía Atómica, CONICET, (1650) San Martín, Argentina*

<sup>2</sup>*Departamento de Física, Universidad de Buenos Aires, Ciudad Universitaria Pabellón I, (1428) Buenos Aires, Argentina*

(Received 17 August 2012; published 17 May 2013)

In this Letter, we find by means of first-principles calculations a new physical mechanism to generate a two-dimensional electron gas, namely, the breaking of charge ordering at the surface of a charge-ordered semiconductor due to the incomplete oxygen environment of the surface ions. The emergence of the 2D gas is independent of the presence of oxygen vacancies or polar discontinuities; this is a self-doping effect. This mechanism might apply to many charge-ordered systems, in particular, we study the case of BaBiO<sub>3</sub>(001). Our calculations show that the outer layer of the Bi-terminated simulated surface turns more cubiclike and metallic while the inner layers remain in the insulating monoclinic state that the system present in the bulk form. On the other hand, the metallization does not occur for the Ba termination, a fact that makes this system appealing for nanostructuring. Finally, in view of the bulk properties of this material under doping, this particular finding sets another possible route for future exploration: the potential scenario of 2D superconductivity at the BaBiO<sub>3</sub> surface.

DOI: [10.1103/PhysRevLett.110.206805](https://doi.org/10.1103/PhysRevLett.110.206805)

PACS numbers: 73.20.-r, 71.15.Mb, 71.30.+h, 71.45.Lr

When the extension of a semiconductor crystal is not assumed infinite, due to the presence of a surface or an interface with another material, the bulk electronic wave functions are altered giving rise to intrinsic surface states that are allowed to lie in the band gap. These surface states might have metallic behavior conforming a two-dimensional electron gas (2DEG). The emergence of these 2DEGs at the interface of conventional semiconductors has been at the basis of device development and engineering in the field of electronics for more than 50 years. The physical mechanism behind the generation of these conducting states may have different origins depending on the system. At clean undoped semiconducting surfaces, they can be attributed to the unpaired electrons of dangling bond states within the band gap, while, in semiconductor heterojunctions, band bending is a determinant factor for 2DEG formation [1].

Since the last decade, due to the progress made in the heteroepitaxial growth of complex oxides, it has become possible to generate 2DEGs at oxide interfaces [2]. This fact brought about a wide variety of phenomena such as superconductivity [3], magnetic order [4], and electron correlation-driven effects [5], among others, awakening the interest on both fundamental issues and their future technological applications in the field of oxide electronics. It is nowadays still an issue of intense debate what is the origin of the 2DEGs at these oxide interfaces. One point of view ascribes them to polar-nonpolar interfaces and is based on the polar “catastrophe” model that proposes an electronic reconstruction to compensate the growing dipole moment as the number of polar layers increases. Another invoked mechanism is the presence of oxygen vacancies

in the substrate. Each scenario explains part of the story [2,6–8] and, probably, a complete understanding of the intrinsic nature of the 2DEG formation is highly dependent on the materials involved and on the experimental setup. Recently, it has been shown that a 2DEG can also be generated in a simpler context, namely, at the vacuum-cleaved surface of SrTiO<sub>3</sub>. In this case, a metallic gas is formed independently of the oxide bulk carrier densities, opening the way towards novel means of 2DEG generation at the surface of transition-metal oxides [9]. In this case, the presence of oxygen vacancies is suggested to lie behind the emergence of metallic surface states.

In this Letter, based on density functional theory (DFT) calculations [10], we propose not only a new candidate that is able to sustain a confined electron gas but also a new physical mechanism to generate it that is different from the ones invoked until now. We show, namely, that a 2DEG is formed at the (001) surface of insulating BaBiO<sub>3</sub> as a consequence of a charge-order disruption. No external factors, such as polar discontinuities or oxygen vacancies, are necessary to obtain, in this case, the 2DEG except for the Bi-terminated surface itself. The surface generated carrier densities are quite high and of the same order of magnitude as the ones measured at other oxide interfaces or clean surfaces. This phenomenon might be present in many other charge-ordered materials as will be discussed later.

In order to understand the nature of our finding, we briefly describe the phase diagram of bulk BaBiO<sub>3</sub>. At high temperature ( $T > 750$  K) it is a cubic perovskite exhibiting metallic behavior. Formally, one would expect each bismuth to have a valence  $4+$ . However, Bi is a typical valence-skipping atom, and even in the high

temperature metallic phase, it presents charge disproportionation. At lower temperatures, this disproportionation couples to the tilting of the  $\text{BiO}_6$  octahedra. The crystal structure goes through a rhombohedral phase ( $750 \text{ K} > T > 405 \text{ K}$ ), becoming monoclinic for  $T < 405 \text{ K}$  [11]. The charge disproportionation together with the structural distortion are further enhanced giving rise to a formal  $\text{Bi}^{5+}\text{-Bi}^{3+}$  charge-ordered Peierls-like insulator in the low temperature monoclinic phase. The oxygen octahedra around the Bi ions present alternating breathing-in and breathing-out structural instabilities. Being that the electronic properties of this material are fascinating by themselves, the discovery of high- $T_c$  superconductivity in doped  $\text{BaBiO}_3$  [12,13] makes this system even more intriguing and interesting. It has been shown that upon doping, the monoclinic phase turns cubic or tetragonal (depending on the dopant) and metallic, exhibiting superconductivity with  $T_c$ 's as high as 30 K. Much of the understanding of the electronic structure and structural properties of both, the parent  $\text{BaBiO}_3$  and the doped compounds, has been accomplished by means of first-principles calculations [14–16]. In this material, the physics is dominated by spatially quite extended  $\text{Bi}(s)\text{-O}(p)$  orbitals. In the absence of important correlation effects, as in typical  $d$  or  $f$  electron systems, much progress has been made from early local-density approximation (LDA) calculations [17] based on DFT.

Calculations using LDA [or the generalized-gradient approximation (GGA) [18]] could already explain the splitting of the  $\text{Bi}(s)\text{-O}(p)$  band around  $E_F$  due to Peierls-like distortions that are switched on, in particular, by the breathing instability [16]. These calculations account, then, for the charge disproportionation and its relation to the structural distortions in the monoclinic phase. LDA (GGA) results predict a semimetallic behavior; however, it is well known that  $\text{BaBiO}_3$  bulk presents an indirect gap whose experimental reported value goes from 0.2 eV to 1.1 eV [19]. More recently it has been shown that in order to open the indirect gap and describe quantitatively the structural properties and the insulating behavior of this phase of bulk  $\text{BaBiO}_3$ , it is necessary to go beyond standard DFT approaches, for instance, by using hybrid functionals that combine a fraction of nonlocal exact exchange with local or semilocal approximations [20].

In this contribution, the theoretical study of the (001) surface of  $\text{BaBiO}_3$  is faced for the first time. We perform first-principles DFT calculations and take care of the gap problem by cross-checking the results with functionals that go beyond LDA or GGA such as the modified Becke-Johnson potential (MBJ) [21] and the Heyd-Scuseria-Ernzerhof (HSE) hybrid functional [22]. The MBJ correction is done within the WIEN2K code [23] and the HSE functional within the VASP package [24]. In the Supplemental Material [25], we show that the main physical findings are obtained using either GGA, MBJ, or HSE functionals. The surfaces are modeled by supercells with

different slab thicknesses. We consider slabs composed of 9 to 15 layers that are stacked following the monoclinic crystal structure with both Ba- and Bi-terminated situations in the (001) direction. To avoid the interaction between opposite surfaces, they are separated in the  $z$  direction by an empty space volume ranging from 9 to 21 Å. The supercells have two inversion symmetric surfaces for simplicity. All internal atomic positions are allowed to relax.

Our calculations indicate that Bi-terminated  $\text{BaBiO}_3$  turns metallic while the Ba-terminated surface remains insulating as in the bulk (monoclinic phase). The results obtained for different supercells with a different number of layers are qualitatively the same in the corresponding termination. The comparison among different slabs is useful to detect finite size effects (as described below).

In Fig. 1 we show the band structure and total densities of states (DOSs) for a Ba- and a Bi-terminated slab, Figs. 1(a) and 1(b), respectively. These band structures correspond to slabs with 11 and 13 layers. In the band structure plots, the bulk projected bands in the (001) direction, depicted in light gray (red) in the (001) direction are shown on top of the ones coming from the slab calculations, depicted in dark gray (blue). It can be clearly seen that in the first case, the system behaves as an insulator, while in the second one there are several surface states crossing  $E_F$ , giving rise to metallic behavior. In Fig. 1(a), the bands above the Fermi level have mainly  $\text{Bi}^{5+}\text{-O}$  character and the ones below have mainly  $\text{Bi}^{3+}\text{-O}$  character. The set of bands below  $-2.0$  eV have mostly O- $p$  states with a significant Bi- $6s$  weight. In Fig. 1(b), there are four bands (surface states) crossing  $E_F$  that basically come from the Bi surface atoms which are strongly mixed with O- $p$  states. There are also visible surface states around  $-2.0$  eV due to this hybridization. There is a tiny pocket around the  $M$  point which is due to a finite size effect. The contribution of this pocket to the Fermi surface increases considerably for thinner slabs.

The metallization of the Bi-terminated surface is a consequence of the incomplete octahedral environment of the Bi ions, which produces a rearrangement of the charge

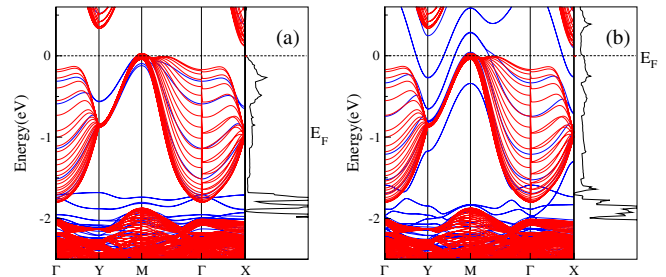


FIG. 1 (color online). Band structure and total density of states obtained using GGA with the MBJ correction for (a) Ba-terminated and (b) Bi-terminated  $\text{BaBiO}_3$  (001). The light gray or red (dark gray or blue) bands are the bulk projected (slab) band structure. The corresponding DOS plots are inverted, energy vs DOS (up to 30 1/eV).

distribution suppressing the charge ordering at that  $\text{BiO}_2$  plane. This suppression of the disproportionation is, in fact, partial but strong enough to turn the system metallic, as it is the case in the high temperature cubic phase of bulk  $\text{BaBiO}_3$ . On the other hand, for Ba termination, the oxygen octahedral environment of all Bi ions is complete, and the charge ordering is then not affected in any of the  $\text{BiO}_2$  planes. There is, indeed, a slight charge redistribution among the O atoms at the BaO surface plane, which has no effect on the insulating behavior of the whole system.

In order to trace the origin of this metallicity, in Fig. 2 we plot the DOSs (obtained with the MBJ correction) projected onto the  $\text{BiO}_2$  planes for the Bi-terminated 13-layer slab. The BaO layers are skipped for the sake of simplicity. The bulk projected DOSs are plotted on top of the ones of layer 4 (in black) for comparison. The effects of charge disproportionation in the bulk can be clearly observed within the  $[-2 \text{ eV}, 2 \text{ eV}]$  energy range. There are quasisymmetrically distributed occupied and empty  $6s$  bands around  $E_F$ , presenting the  $\text{Bi}^{3+}$  ions' mostly occupied states and the  $\text{Bi}^{5+}$  ions' mostly empty ones. The important  $\text{Bi}(6s)\text{-O}(p)$  hybridization is clearly appreciable in the O projected DOS.

Our slab results show that already the third Bi layer from the surface has a bulklike projected DOS. The slight downward shift of the Fermi level for layers 3 and 4, as compared to the bulk, is again due to a finite size effect. The thinner the slab, the larger the downward shift of  $E_F$  into the  $6s$  valence bands. The behavior of the Bi- $6s$  and O states of the surface and subsurface Bi layers (labeled as 1 and 2) is qualitatively different to what happens in the

deeper Bi planes. In layers 1 and 2 there is an effective charge transfer from the originally  $\text{Bi}^{3+}$  to the  $\text{Bi}^{5+}$  ions. The system turns, in this way, metallic and this metallicity is mainly confined to the two outer  $\text{BiO}_2$  planes of the Bi-terminated  $\text{BaBiO}_3$ . For the thinner film considered, namely, the nine-layer slab (not shown in Fig. 2), the confinement is less effective but still the metallization is predominantly at the outer layers.

In Fig. 3 we show a scheme of the physical mechanism explaining the 2DEG formation. The band structure of the bulk monoclinic phase presents one fully occupied and one unoccupied band per formula unit, just below and above  $E_F$ , composed by hybridized  $sp$  states that can be described with  $\text{Bi}(6s)\text{-O}(2p)$   $\sigma$  orbitals centered around the  $\text{Bi}^{3+}$  and  $\text{Bi}^{5+}$ , respectively [14]. Taking into account that each Bi ion has six O nearest neighbors and that the occupied band (with mainly  $\text{Bi}^{3+}\text{-O}$  character) has occupation  $N = 2$ , we can estimate that each bond contributes with  $\Delta \sim 2/6 = 0.33$  electrons. On the other hand, the empty band associated with an  $sp\sigma$  orbital centered around the  $\text{Bi}^{5+}$  ion implies that there has been a charge transfer,  $\Delta$ , from the  $\text{Bi}^{5+}$  site to the six neighbors [Fig. 3(a)]. In the clean Bi-terminated surface, the extra charge that was being exchanged with the now missing BaO layer  $2\Delta$  is redistributed in the surface layer. The flux of charge is now inverted; the band with mainly  $\text{Bi}^{5+}\text{-O}$  character gets filled by around  $\Delta$  electrons while the band with  $\text{Bi}^{3+}\text{-O}$  character loses approximately the same amount of charge. This effect brings about one electron and one hole pockets in the Fermi surface. We can validate this simple picture by calculating the 2D carrier density,  $n_{2D}$ , through Luttinger's theorem

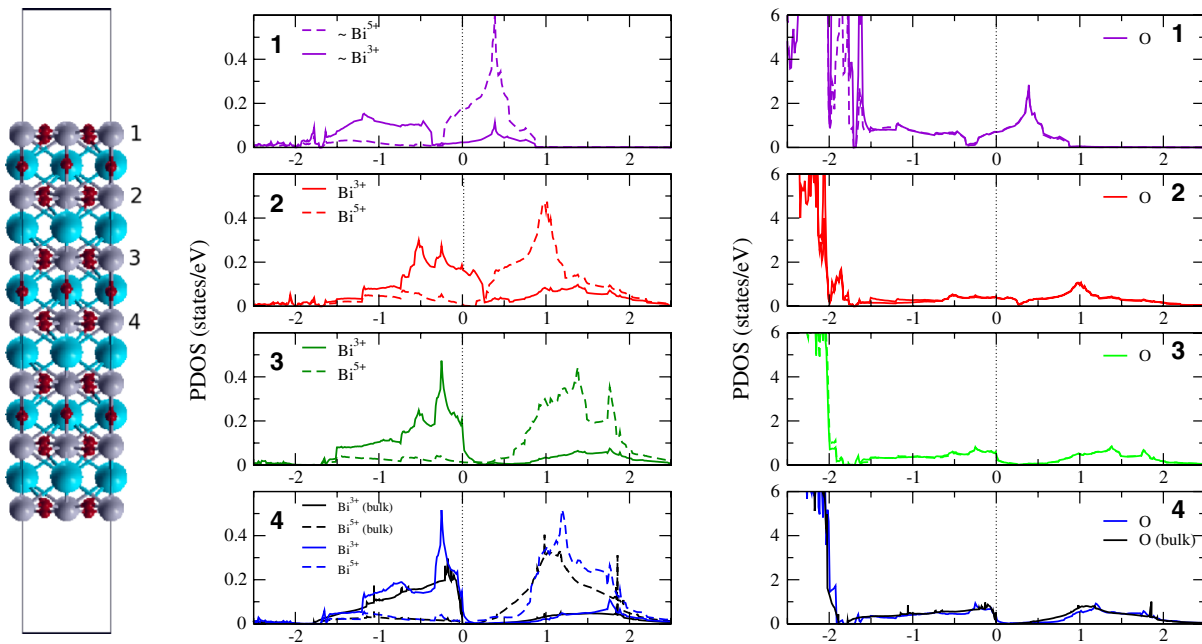


FIG. 2 (color online). To the left, the simulated 13-layer slab with the  $\text{BiO}_2$  planes labeled from 1 to 4. The projected DOSs on these planes are in the central and right plots for the Bi- $s$  and O projected states, respectively. On top of the DOSs of layer 4, the corresponding bulk projected DOSs are plotted (monoclinic phase) for comparison.  $E_F$  is at 0 eV.

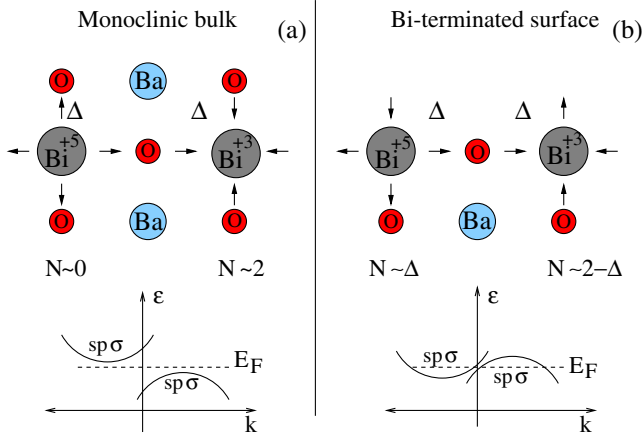


FIG. 3 (color online). Schematic representation of the physical mechanism originating the 2DEG at the Bi-terminated  $\text{BaBiO}_3$  (001) surface.  $2\Delta$  is the charge difference between the two  $sp\sigma$  orbitals around each Bi ion type in the charge-ordered monoclinic phase.

(see the Supplemental Material [25]). We obtain  $n_{2D} = 0.62$  charge carriers per 2D unit cell for the Bi-terminated 13-layer slab, which agrees quite well with the estimated value of  $2\Delta \sim 0.66$  [26]. It should be stressed that the calculated carrier density is of the same order of magnitude as the one estimated for sharp  $\text{LaAlO}_3/\text{SrTiO}_3$  interfaces and cleaved  $\text{SrTiO}_3$  surface [8,9].

The charge redistribution at the Bi-terminated surfaces is present even in the unrelaxed systems, which turn metallic just by bond breaking (see the Supplemental Material [25] for unrelaxed cases). When the slabs are allowed to relax, the breathing distortions are washed out at the surface and subsurface Bi planes, contributing to an enhancement of the surface metallicity. In the deeper layers, compressed and expanded octahedra remain without significant changes, preserving there the insulating charge ordering as in the bulk. In Fig. 4 we plot the average Bi-O bond length [Fig. 4(a)] and the difference of the atoms in molecules (AIM) charges [27] of the  $\text{Bi}^{3+}$  and  $\text{Bi}^{5+}$  ions,  $\delta_{\text{AIM}}$  [Fig. 4(b)], at each layer for the 13-layer slab obtained with GGA. We observe that both quantities evolve from a monocliniclike situation in the core of the slab, to a cubicle one in the surface. There is experimental evidence from thin film measurements supporting these results [28].

We can draw a parallelism between the effect of the surface on the structural and electronic properties of the Bi-terminated film and the effect of temperature on the same properties in bulk  $\text{BaBiO}_3$ . That is, we could think of having “cold” insulating monoclinic regions in the deeper planes and “hot” metallic cubic ones close to the surface. We can also make an analogy with the high- $T_c$  superconductor, the doped  $\text{BaBiO}_3$  in bulk, which turns cubic and metallic upon doping with K or Pb. In this context, the predicted 2DEG at the  $\text{BiO}_2$  surface deserves further investigation regarding its superconducting properties.

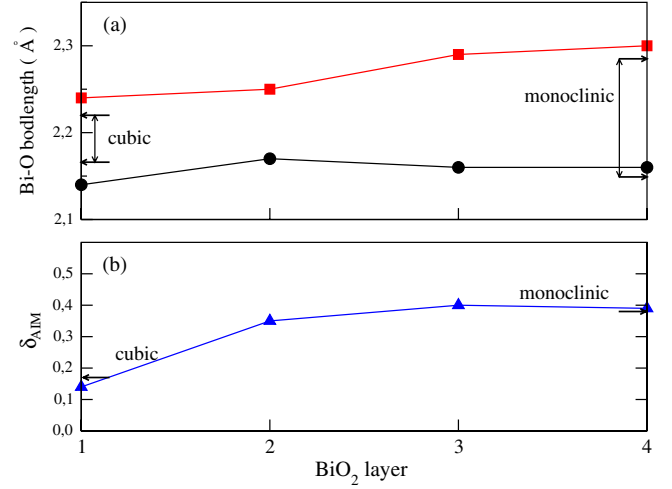


FIG. 4 (color online). (a) Average Bi-O bond lengths for the two types of Bi sites obtained for the 13-layer Bi-terminated  $\text{BaBiO}_3$  slab. Squares (circles) correspond to the  $\text{Bi}^{3+}\text{-O}$  ( $\text{Bi}^{5+}\text{-O}$ ) bond lengths, respectively. (b)  $\delta_{\text{AIM}}$ , the AIM charge difference between the two Bi ions in each layer. The arrows indicate the corresponding calculated values for low- $T$  monoclinic and high- $T$  cubic bulk phases.

Another interesting finding with potential technological applications is the fact that the  $\text{BaO}$  surface is insulating. The possibility of *drawing*  $\text{BiO}_2$  nanocircuits on top of  $\text{BaO}$ -terminated  $\text{BaBiO}_3$  surfaces constitutes a subject appealing for exploration. Finally, this surface metalization phenomenon might be present in many other charge-ordered materials. Potential candidates deserving further investigation are  $\text{CaFeO}_3$  [29],  $\text{Pb}_2\text{O}_3$  [30], and  $\text{LuNiO}_3$  [31].

Summarizing, in this Letter we propose a new physical mechanism to generate a two-dimensional electron gas at the surface of charge-ordered insulators. It is based on the charge-order breaking of the disproportionated ions at these surfaces. In particular, we study the case of  $\text{BaBiO}_3(001)$  by means of first-principles calculations and predict the formation of a 2DEG for Bi termination. The obtained metallic state is confined to the outer layers and presents a quite high 2D carrier density, of the order of 0.6 electrons per 2D unit cell. This phenomenon is probably not exclusive of  $\text{BaBiO}_3$  and might occur in other charge-ordered semiconductors. It is independent of any external factor such as the ambient oxygen pressure or polar discontinuities, making this system a self-doping surface with promising potential applications to oxide electronics.

The authors thank A. Santander-Syro and M. Rozenberg for suggesting to us the problem hereby studied. We also thank both of them and R. Weht for illuminating discussions. The calculations were performed using the ISAAC cluster at the computer center of DCAP-GTIC, CACNEA. This work received financial support through PICT-R No. 1776, PIP No. 0258, and UBACyT No. X123.

- [1] M. Lannoo and P. Friedel, *Atomic and Electronic Structure of Surfaces: Theoretical Foundations* (Springer-Verlag, Berlin, 1991); Z. Zhang and J. T. Yates, Jr., *Chem. Rev.* **112**, 5520 (2012).
- [2] A. Ohtomo and H. Y. Hwang, *Nature (London)* **427**, 423 (2004).
- [3] N. Reyren *et al.*, *Science* **317**, 1196 (2007).
- [4] A. Brinkman, M. Huijben, M. van Zalk, J. Huijben, U. Zeitler, J. C. Maan, W. G. van der Wiel, G. Rijnders, D. H. A. Blank, and H. Hilgenkamp, *Nat. Mater.* **6**, 493 (2007).
- [5] R. Pentcheva and W. E. Pickett, *Phys. Rev. Lett.* **99**, 016802 (2007).
- [6] A. Kalabukhov, R. Gunnarsson, J. Börjesson, E. Olsson, T. Claeson, and D. Winkler, *Phys. Rev. B* **75**, 121404 (2007).
- [7] G. Herranz *et al.*, *Phys. Rev. Lett.* **98**, 216803 (2007).
- [8] M. Basletic, J.-L. Maurice, C. Carrétero, G. Herranz, O. Copie, M. Bibes, É. Jacquet, K. Bouzehouane, S. Fusil, and A. Barthélémy, *Nat. Mater.* **7**, 621 (2008).
- [9] A. F. Santander-Syro *et al.*, *Nature (London)* **469**, 189 (2011).
- [10] P. Hohenberg and W. Kohn, *Phys. Rev.* **136**, B864 (1964).
- [11] D. Cox and A. Sleight, *Solid State Commun.* **19**, 969 (1976).
- [12] A. W. Sleight, J. L. Gillson, and P. E. Bierstedt, *Solid State Commun.* **17**, 27 (1975).
- [13] R. J. Cava, B. Batlogg, J. J. Krajewski, R. Farrow, L. W. Rupp, A. E. White, K. Short, W. F. Peck, and T. Kometani, *Nature (London)* **332**, 814 (1988).
- [14] L. F. Mattheiss and D. R. Hamann, *Phys. Rev. B* **28**, 4227 (1983); *Phys. Rev. Lett.* **60**, 2681 (1988).
- [15] A. I. Liechtenstein, I. Mazin, C. Rodriguez, O. Jepsen, O. Andersen, and M. Methfessel, *Phys. Rev. B* **44**, 5388 (1991); K. Kunc, R. Zeyher, A. I. Liechtenstein, M. Methfessel, and O. K. Andersen, *Solid State Commun.* **80**, 325 (1991); V. Meregalli and S. Y. Savrasov, *Phys. Rev. B* **57**, 14453 (1998).
- [16] T. Thonhauser and K. M. Rabe, *Phys. Rev. B* **73**, 212106 (2006).
- [17] J. P. Perdew and A. Zunger, *Phys. Rev. B* **23**, 5048 (1981).
- [18] J. P. Perdew, K. Burke, and M. Ernzerhof, *Phys. Rev. Lett.* **77**, 3865 (1996).
- [19] See Ref. [20] and references therein.
- [20] C. Franchini, A. Sanna, M. Marsman, and G. Kresse, *Phys. Rev. B* **81**, 085213 (2010).
- [21] F. Tran and P. Blaha, *Phys. Rev. Lett.* **102**, 226401 (2009).
- [22] J. Heyd, G. Scuseria, and M. Ernzerhof, *J. Chem. Phys.* **118**, 8207 (2003); A. V. Krukau, O. A. Vydrov, A. F. Izmaylov, and G. E. Scuseria, *J. Chem. Phys.* **125**, 224106 (2006).
- [23] P. Blaha *et al.*, *WIEN2K, An Augmented Plane Wave Plus Local Orbitals Program for Calculating Crystal Properties* (Vienna University of Technology, Vienna, Austria, 2002).
- [24] G. Kresse and J. Furthmüller, *Comput. Mater. Sci.* **6**, 15(R) (1996); J. Paier, R. Hirschl, M. Marsman, and G. Kresse, *J. Chem. Phys.* **122**, 234102 (2005).
- [25] See Supplemental Material <http://link.aps.org/supplemental/10.1103/PhysRevLett.110.206805> for details on the results obtained with different functionals, the calculation of the 2D carrier density, and relaxation effects.
- [26] In this work, we study the stoichiometric surface. A deeper analysis of the effect of oxygen vacancies is in general necessary for oxide perovskites. However, simple arguments as the ones described above (Fig. 3) can be used to anticipate the robustness of the proposed mechanism in the presence of oxygen vacancies.
- [27] R. F. W. Bader, *Atoms in Molecules: A Quantum Theory* (Oxford University Press, New York, 1990).
- [28] H. Guyot, C. Filippini, and J. Marcus, *J. Alloys Compd.* **195**, 543 (1993).
- [29] V. E. Alexandrov, E. A. Kotomin, J. Maier, and R. A. Evarestov, *J. Chem. Phys.* **129**, 214704 (2008).
- [30] W. A. Harrison, *Phys. Rev. B* **74**, 245128 (2006).
- [31] I. I. Mazin, D. I. Khomskii, R. Lengsdorf, J. A. Alonso, W. G. Marshall, R. M. Ibberson, A. Podlesnyak, M. J. Martínez-Lope, and M. M. Abd-Elmeguid, *Phys. Rev. Lett.* **98**, 176406 (2007).